

Boundary Effects on the Structural Stability of Stationary Patterns in a Bistable Reaction-Diffusion System

G. G. Izús,¹ J. Reyes de Rueda,¹ and C. H. Borzi^{2, 3}

Received June 17, 1997; final August 20, 1997

We study a piecewise linear version of a one-component, two-dimensional bistable reaction-diffusion system subjected to partially reflecting boundary conditions, with the aim of analyzing the structural stability of its stationary patterns. Dirichlet and Neumann boundary conditions are included as limiting cases. We find a critical line in the space of the parameters which divides different dynamical behaviors. That critical line merges as the locus of the coalescence of metastable and unstable nonuniform structures.

KEY WORDS: Hot-spot model; reaction-diffusion; structural stability; non-equilibrium potential; albedo BCs.

1. INTRODUCTION

The subject of pattern formation in extended dissipative systems has become a very active field of research, from both the experimental and theoretical points of view. In particular, the description of dissipative structures in terms of reaction-diffusion (RD) equations has been a very fecund source of tractable models in physics, chemistry, and biology.⁽¹⁻⁹⁾

The boundary conditions (BCs) determine the merging and the stability of nonequilibrium structures in RD systems.⁽¹⁰⁻¹⁵⁾ In recent papers, we have studied the role of the BCs for one- and two-component systems.⁽¹⁴⁻¹⁸⁾

¹ Departamento de Física, Facultad de Ciencias Exactas y Naturales, Universidad Nacional de Mar del Plata, Deán Funes 3350, (7600) Mar del Plata, Argentina.

² MONDITEC S.A., Olazabal 1927, (1428) Buenos Aires, Argentina.

³ To whom correspondence should be addressed.

The specific model we shall study here belongs to a family of one-component models with a broad range of applicability, whose general formulation reads^(7, 19)

$$\frac{\partial T(\mathbf{r}, t)}{\partial t} = D \nabla^2 T + F(T) \quad (1)$$

Here D is the diffusion coefficient, $T(\mathbf{r}, t)$ is a real field representing the physical magnitude of interest which in our case will be the temperature, and the local term $F(T)$ accounts for the dynamics of the system in the absence of diffusion. For bistable RD systems $F(T)$ is the reaction term and takes the form of a cubic-like function. Among its three roots, two are stable fixed points and the other one is unstable.^(7, 9)

We shall concentrate on a bistable reaction-diffusion system subjected to partially reflecting boundary conditions (albedo BCs). This type of BC links the value of the field to its normal derivative at the boundary Σ through the value of the albedo parameter $k > 0$:

$$\left. \frac{\partial T}{\partial n} \right|_{\Sigma} = -kT|_{\Sigma} \quad (2)$$

meaning that the boundary Σ is partially reflective. Albedo BCs are currently used to simulate partially reflecting boundaries for heat flux.^(20, 21) These BCs can be achieved in chemical reactions by means of a controlled flux of species at the boundaries in an unstirred reactor tank limited by gel strips.^(22–25) In refs. 13, and 15–18 it was shown that under certain circumstances this type of BC can control the relative stability between the attractors of RD systems. The usual Dirichlet and Neumann BCs (complete absorption or reflection at the boundaries, respectively) correspond to the limiting cases $k \rightarrow \infty$ and $k \rightarrow 0$.

We shall focus on a bidimensional one-component model of an electrothermal instability called the Ballast resistor. This system admits a description in terms of a bistable RD equation.^(10, 26–29) For the sake of clarity we shall restrict our analysis to the superconducting version of the resistor, described by the so-called “hot-spot” model. That device is currently used in superconducting microbridges.⁽³⁰⁾ After a suitable rescaling of the variables, the balance equation can be written as the following piecewise linear bistable RD equation:

$$\frac{\partial T(r, t)}{\partial t} = \nabla^2 T - T + \theta[T - T_{ch}] \quad (3)$$

where T is the scaled temperature field which determines the state of the system, θ is the Heaviside step function, and T_{ch} is an activation threshold representing the scaled critical temperature of the superconductor ($0 < T_{ch} < 1$). Equation (3) models a realistic bistable RD system, keeps its qualitative characteristics, and allows us to obtain analytical results. In particular, exact stationary solutions can be explicitly found. The formation of a nonuniform stable structure in this model system is interpreted as a nucleation phenomenon as follows: The unstable pattern is the nucleation fluctuation and the uniform solution is the metastable phase.

We point out that most of the results obtained for this piecewise linear model could be straightforwardly extended to more general cases with smoother bistable potentials, since it has already been verified that the piecewise linear approximation preserves the essentials of the phase behavior.^(18,31–34) In Eq. (3), the piecewise linear reaction term is a consequence of the superconducting nature of the resistor. In a more general context, discontinuous force terms with piecewise continuous derivatives typically result from singular perturbations of two-component systems with one vanishing diffusion constant.⁽³⁵⁾

We shall see how the BCs and the value of the activation threshold determine the region in the space of the parameters where the piecewise linear RD system modeled by Eq. (3) shows a bistable regime. In particular, we want to elucidate (a) the structural stability of dissipative structures subject to Dirichlet and Neumann BCs, and (b) the effect of a finite reflectivity on the coalescence of metastable and unstable structures for different activation thresholds. We shall identify the region in the (T_{ch}, k) space where small variations of those parameters induce a qualitative change in the nature of the dynamics. Our analysis will be carried out by exploiting the notion of the nonequilibrium potential of the system. That approach offers a way of revisiting problems that have recently attracted attention both experimentally and theoretically, namely the effect of the BCs on the pattern selection process, the induction of transitions by fluctuations, the possibility of the propagation of solitary traveling waves in chemical reactions, etc.^(36–42)

To simplify further, we consider here the symmetric case in which the albedo parameter k takes a single value on the convex boundary, and we use that value as a control parameter. The generalization of the present analysis to angle-dependent BCs is currently under study.

2. PATTERN FORMATION IN THE BALLAST RESISTOR

We review in this section the axially symmetric stationary patterns of Eq. (3) in two spatial dimensions.⁽¹⁶⁾ The scaled equation for the

temperature field reads

$$\left(\frac{d^2}{dr^2} + \frac{1}{r} \frac{d}{dr}\right) T - T + \theta[T - T_{ch}] = 0 \quad (4)$$

where $r = |\mathbf{r}|$. In what follows, we consider Eq. (4) restricted to the finite region $r \leq R_L$ and subject to partially reflecting BCs at $r = R_L$.

2.1. Stationary Patterns

We consider patterns of two regions with circular symmetry: the central region ($r < R_c$) is above the scaled threshold temperature T_{ch} (activated), and the surrounding annulus is below T_{ch} (not activated). Figure 1 shows the profiles of two typical patterns associated with the same values of T_{ch} and k .

Equation (4) is solved by proposing different analytical forms for $T(R)$ (here these are linear combinations of zeroth order modified Bessel functions), depending on whether $T > T_{ch}$ or $T \leq T_{ch}$. These expressions, as well as their first derivatives, have to be matched at the spatial coordinate of the boundary between the activated and the not-activated regions (matching points), which we denote generically by R_c . In order to identify R_c , the equation $T(R_c(k)) = T_{ch}$ must be solved numerically. Figure 2

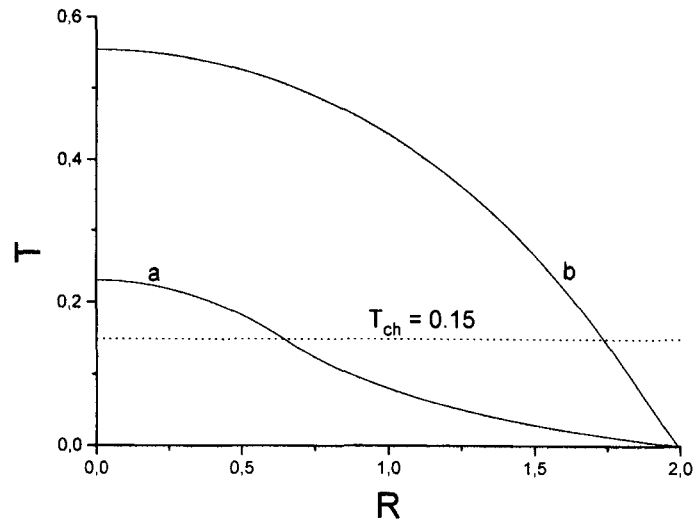


Fig. 1. Typical dissipative stationary structures for the “hot-spot” model. The values of the parameters are $T_{ch} = 0.15$ (dotted line), $k = 8$, and $R_c = 0.651$ (curve a) and $R_c = 1.838$ (curve b).

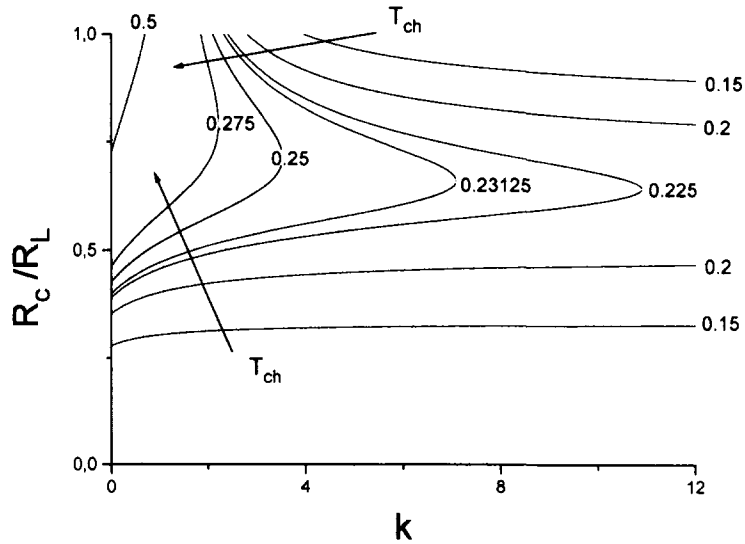


Fig. 2. R_c/R_L vs. the albedo parameter k . The curves are parametrized with the values of T_{ch} , and $R_L = 2$ has been fixed throughout. The double-valued curves cannot be resolved numerically around the diverging slope points. The arrows indicate the sense in which T_{ch} increases.

shows some general features of the solutions of that implicit equation for different values of T_{ch} . The curves are parametrized with the values of T_{ch} , and $R_L = 2$. There are three types of curves: monotonically increasing ones (which exist for small k and high T_{ch}), closed branches, and open branches. For the open branches, in the limit $k \rightarrow \infty$ we recover Dirichlet BCs. The nonequilibrium potential determines the dynamics of the system and the nature of the branches (closed or open).

For each value of T_{ch} there exists a threshold value of k , namely k_{\min} , where the upper branches $R_c(k)$ start at the value R_L . Figure 3 shows k_{\min} vs. T_{ch} . For $k < k_{\min}$ the structures associated with the upper branches remain above T_{ch} , so there is not an associated R_c for them. For $k \rightarrow 0$, i.e., Neumann BCs, the structures associated with the upper branches tend to the uniform stable solution $T = 1$.

2.2. Local Stability

The standard linear stability analysis⁽¹⁶⁾ shows that the monotonically increasing branches are all unstable. In the case of the open branches, the upper (lower) ones are stable (unstable). For the closed curves we have the

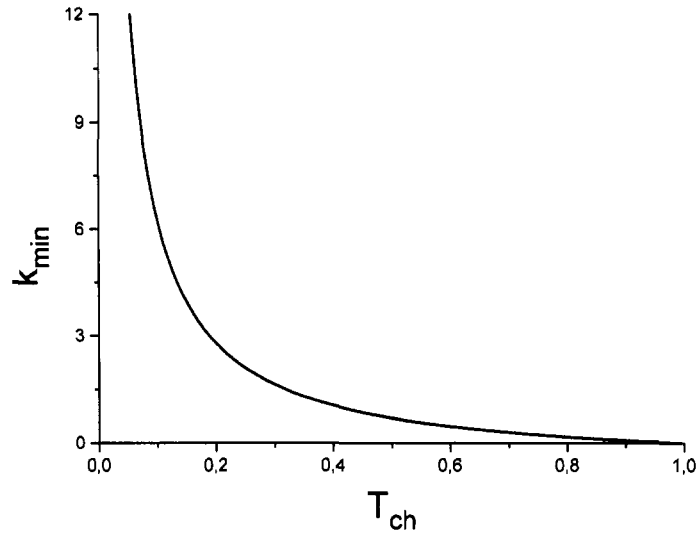


Fig. 3. k_{\min} vs. T_{ch} . For $k < k_{\min}$ the nonuniform structures associated with the upper branches in Fig. 2 remain above T_{ch} . For $k \geq k_{\min}$ we have a two-folded solution where only the upper branch corresponds to a stable pattern.

same situation when considering them as divided into upper and lower branches at the points where their slopes diverge. The locus of those dividing points determines a line of marginal stability. The stationary homogeneous solution $T=0$ is locally stable for all values of T_{ch} and k (it is a homogeneous attractor).⁽¹⁶⁾

2.3. Global Stability

We shall use the nonequilibrium potential functional to discriminate between stable and metastable states.^(7, 15, 36) For Eq. (3), that functional is defined as

$$\mathbf{U}\{T(\mathbf{r}, t)\} = \int \left\{ \frac{1}{2}(\nabla T)^2 - G(T) \right\} d\sigma + S_{\mathcal{E}} \quad (5)$$

where

$$G[T(\mathbf{r}, t)] = \int_0^T \left\{ -\hat{T} + \theta[\hat{T} - T_{ch}] \right\} d\hat{T} \quad (6)$$

The integration in Eq. (5) runs over the whole area of the system. The surface term S_{Σ} adjusts the BCs: its value is 0 if the BCs imposed are Dirichlet or Neumann, but in the case of albedo BCs, we have⁽¹⁵⁾

$$S_{\Sigma} = \frac{k}{2} \int_{\Sigma} T^2 d\mathcal{L} \quad (7)$$

with $d\mathcal{L} = R_L d\theta$ ($0 \leq \theta < 2\pi$). By using Eq. (5), we can write Eq. (3) in a gradient form:

$$\frac{\partial T}{\partial t} = -\frac{\delta U\{T\}}{\delta T} \quad (8)$$

and we see that \dot{U} vanishes for stationary distributions and is negative for every other case (it is a Lyapunov functional). During its temporal evolution, U decreases until it reaches one of its minima. The unstable structures are related to extrema of U of the saddle-point type and define the magnitude of the barriers between the different locally stable attractors. The stable stationary solution corresponds to the absolute minimum of U . The other linearly stable solutions correspond to metastable states.

Fluctuations in the steady state can also be described in terms of the functional U . For variational systems, U plays the role of a nonequilibrium potential and determines the stationary probability distribution of the fluctuations. In fact, for Eq. (2) subject to an external additive Gaussian white noise we have

$$P\{T\} \sim \exp[-U\{T\}/g] \quad (9)$$

where g is the noise intensity and $P\{T\}$ is the stationary distribution of probability in the functional space. Small fluctuations around the local minimum T_{stat} are Gaussian, since the expansion of U around it takes the form

$$U\{T_{\text{stat}} + \varepsilon\} = U\{T_{\text{stat}}\} + \frac{1}{2} \int \left(\frac{\delta^2 U}{\delta T^2} \right) \Big|_{T_{\text{stat}}} \varepsilon^2 d\sigma + \dots \quad (10)$$

where the quadratic term dominates the expansion.

Figure 4 shows the behavior of U as a function of k for the open branches of Fig. 2. The upper (lower) branches in Fig. 4 correspond to the lower (upper) branches in Fig. 2. As $U\{0\} = 0$, there exists a region of k where the nonuniform structures are stable and the uniform ones ($T=0$) are metastable. But this situation changes for certain values of T_{ch} , for which $T=0$ is the stable solution. That change in the relative stability

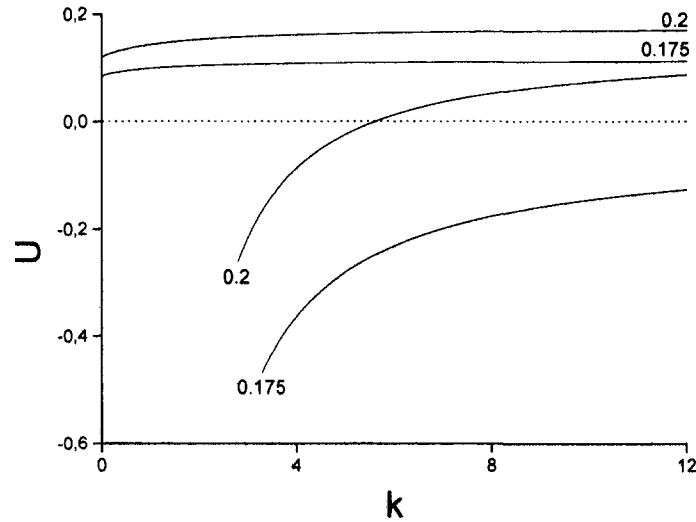


Fig. 4. Nonequilibrium potential vs. the albedo parameter for nonuniform structures. The curves are labeled by their T_{ch} values.

between attractors is induced by tuning the albedo parameter.^(15, 16) The upper branches in Fig. 4 are related to the unstable solutions and correspond to the barriers between stable attractors (saddlepoints of U).

3. CONTROL PARAMETERS

In this section we analyze the structural stability of the dissipative structures introduced above in terms of two control parameters T_{ch} and k . The limits of null reflectivity (Dirichlet BCs) and total reflectivity (Neumann BCs), their environments, and the intermediate values of the reflectivity will be considered separately.

3.1. Dirichlet BCs

Bistability with Dirichlet BCs ($k = \infty$) is only possible for those values of T_{ch} which correspond to the open branches in Fig. 2. Figure 5 shows the variation of R_c with T_{ch} for several values of k . The curve denoted by ∞ corresponds to Dirichlet BCs. There we see that the coalescence of the metastable and the unstable structures occurs when T_{ch} reaches the critical value denoted by $T_{ch}^{(crit)}(\infty)$. The open branches in Fig. 2 correspond to the case $T_{ch} < T_{ch}^{(crit)}(\infty)$. When T_{ch} reaches that critical value, the dissipative

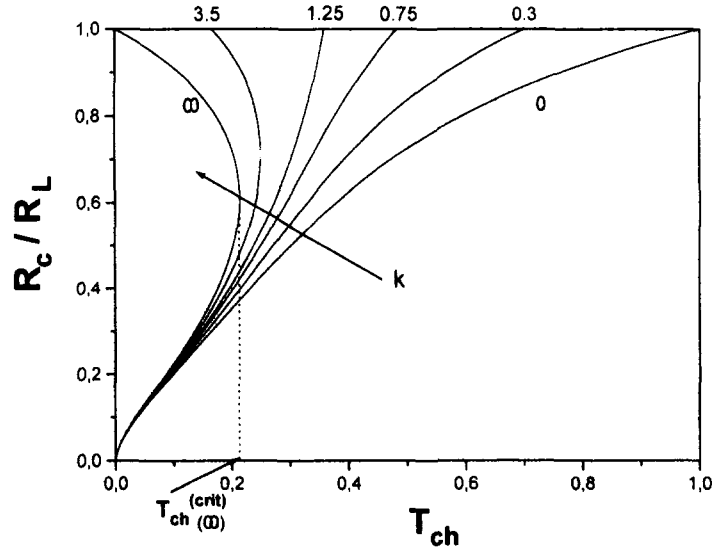


Fig. 5. R_c/R_L vs. T_{ch} for Dirichlet, albedo, and Neumann BCs. The curves are parametrized with k . Dirichlet BCs are indicated by ∞ , and Neumann BCs by 0. For those curves which are double-valued, only the bigger R_c corresponds to a stable pattern. In the vicinity of the diverging slope points we have the same problem as in Fig. 2. The arrow indicates the sense in which the albedo parameter increases.

structures show a structural instability. At that critical point, the dynamics of the system changes from bistable [$T_{ch} < T_{ch}^{(crit)}(\infty)$] to monostable [$T_{ch} \geq T_{ch}^{(crit)}(\infty)$] and the two non-uniform structures collapse.

3.2. Small Reflectivity ($k^{-1} \sim 0$)

In the limit of small reflectivities ($k^{-1} \sim 0$) the structural stability of the stationary patterns can be analyzed by focusing on the behaviour of U . In that parameter region, the nonequilibrium potential takes the form

$$U(k \gg 1) = U(k = \infty) - \frac{1}{2k} \mathcal{L} \frac{I_1^2(R_c)}{I_1^2(R_L)} \quad (11)$$

where \mathcal{L} is the perimeter of the pattern, $I_1(r)$ is the first-order modified Bessel function, and R_c is the matching coordinate corresponding to Dirichlet BCs. In order to obtain Eq. (11) we have considered Eqs. (4) and (5) and the explicit form of the stationary patterns.

As we decrease the albedo parameter (starting from Dirichlet BCs) we induce a more stable structure associated with a diminution of the

nonequilibrium potential. This phenomenon can be extrapolated from Fig. 4. We see from Eq. (11) that in this limit U scales with k^{-1} , and the sign of the correction to the asymptotic value of U gives rise to a stabilization effect on the global properties of the structures.

3.3. Neumann BCs

Neumann BCs do not restrict the allowed values of T_{ch} (as can be appreciated in Fig. 5). In that limit of perfect reflectivity, we have two stable uniform solutions: $T=0$ and $T=1$. The information obtained from the “null-cline analysis”⁽⁷⁾ regarding the nature of the dynamics can be applied directly here. Non-flux boundary conditions show a robust structural stability under changes of the threshold parameter because there is no critical point where the nature of the dynamics of the system could change.

3.4. High Reflectivity ($k \sim 0$)

A small increase of k from Neumann BCs induces a less stable structure whose nonequilibrium potential increases linearly with k . The resulting stable solutions correspond to structures that remain above T_{ch} . In that limit, the nonequilibrium potential associated with those stable patterns takes the simplified form

$$U(k) = -\left[\frac{1}{2} - T_{ch}\right] \mathcal{A} + \frac{k}{1 + k(I_o(R_L)/I_1(R_L))} \mathcal{L} \quad (12)$$

where \mathcal{A} is the area of the pattern. The behavior of U vs. k for these stable structures is depicted in Fig. 6. A scaling behavior is also observed there. In the limit of high reflectivities, we have

$$U(k \ll 1) = U(k=0) + k\mathcal{L} \quad (13)$$

In this case, the sign of the correction to the asymptotic value of U (the surface term) gives rise to a loss of stability on the dissipative structures. This behavior is valid only for $k \ll 1$ and $k < k_{\min}$, because for k small but $k > k_{\min}$ the structures have an exterior annular region which remains below the threshold parameter T_{ch} (patterns with two regions). In Fig. 3 we can see that $k_{\min} \rightarrow 0$ when $T_{ch} \rightarrow 1$.

3.5. Finite Reflectivity

Let us consider now the case of an arbitrary intermediate value of the reflectivity (albedo BCs). The coalescence of the metastable and the

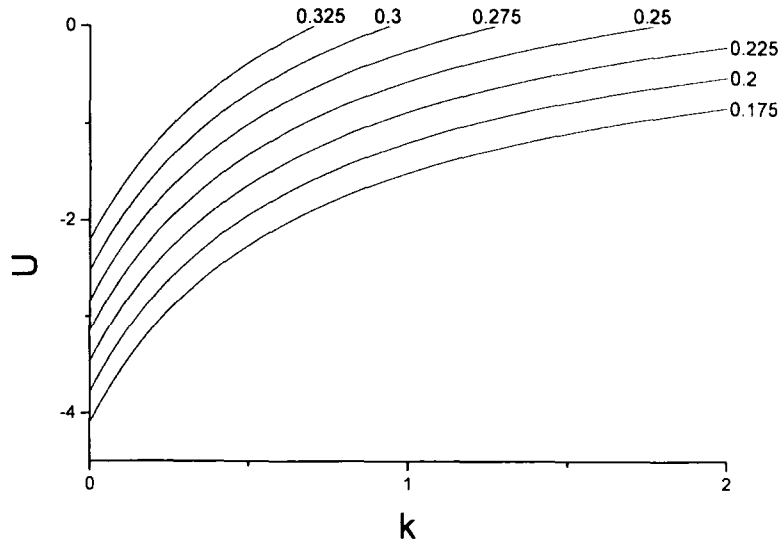


Fig. 6. The nonequilibrium potential for the stationary stable patterns corresponding to the limit of small k . The curves are parametrized by their T_{ch} values.

unstable branches when T_{ch} increases can be seen in Fig. 5. The curves go from double- to single-valued correspondence (in our case the transition occurs for $k \sim 2$). The $T_{ch}^{(crit)}$ is related to k . For small k (single-valued curves), the coalescence occurs with those stable structures which remain above T_{ch} . In that case, the critical value of the threshold corresponds to the intersection of the single-valued curves with the line $R_c = R_L$.

Figure 7 shows the behavior of the nonequilibrium potential as a function of k corresponding to the closed branches. As a general rule U decreases with k , so more reflective boundaries inflate the region where the system exhibits a bistable regime. The coalescence of the stable and the unstable structures gives rise to a cusp in U .

From Figs. 2 and 4 we conclude that there exists a critical line in the space of the parameters (k, T_{ch}) which separates the bistable dynamics from the monostable one. This is the line of marginal stability determined by the points of the closed curves in Fig. 2 [of coordinates $(k, T_{ch}^{(crit)}(k))$] where their slopes diverge. Figure 8 shows that critical line. For $k \rightarrow \infty$ the $T_{ch}^{(crit)}(\infty)$ value is recovered. For T_{ch} below (above) $T_{ch}^{(crit)}(k)$ the dynamics of the system is bistable (monostable). The transition between those different regimes is mediated by the coalescence of the metastable and the unstable structures, which precludes the crisis (extinction) of both structures. In the neighborhood of the critical line, the system exhibits a structural instability under small changes in the values of T_{ch} or k .

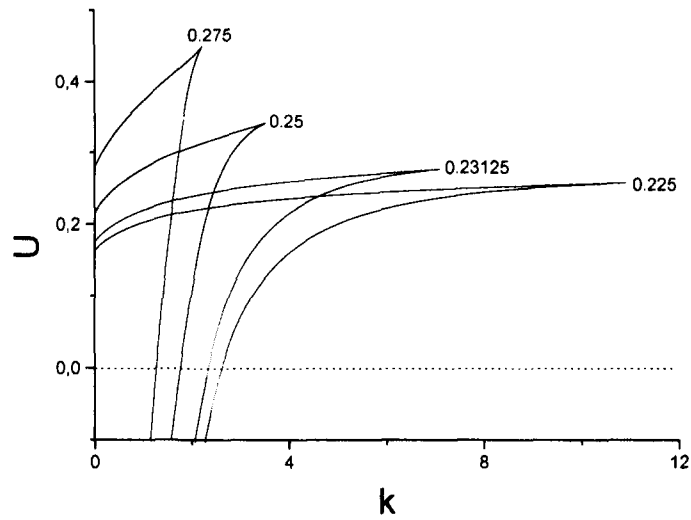


Fig. 7. Nonequilibrium potential vs. the albedo parameter k corresponding to the closed branches in Fig. 2. The curves are labeled by their T_{ch} values. The cusps are the marginal stability points.

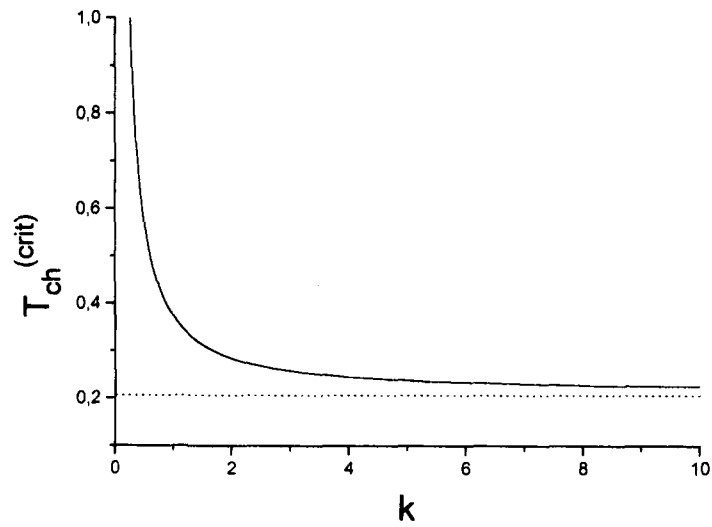


Fig. 8. $T_{ch}^{(crit)}$ vs. k . The dotted line indicates the asymptotic value $T_{ch}^{(crit)}(\infty)$ corresponding to Dirichlet BCs.

4. SUMMARY

We have studied a piecewise linear reaction-diffusion model which represents a bistable system with partially reflecting boundary conditions, with the aim of identifying the region in the parameter space (T_{ch}, k) where the system shows a bistable regime. That region is limited by a critical line which separates the bistable dynamics from a monostable one. At that critical line the system shows a structural instability: the metastable and the unstable nonuniform structures coalesce and produce the collapse of the corresponding attractors.

Tuning the boundary reflectivity is a natural way of selecting a critical value of the threshold temperature. Moreover, in the bistable regime, the barrier between different locally stable attractors depends on the value of the boundary reflectivity. The possibility of tuning the height of that barrier is important, for instance, in phenomena of stochastic resonance in bistable systems.⁽⁴³⁾

In the neighborhood of the Dirichlet BCs ($k \rightarrow \infty$) the structural stability persists far beyond the critical threshold value. The effect of decreasing k is to set a more stable solution. The nonequilibrium potential decreases with k^{-1} in that limit. The structure is stable for T_{ch} small, but that situation changes for bigger activation thresholds. The dissipative bistable systems with $T_{ch} \rightarrow T_{ch}^{(crit)}(\infty)$ and subject to Dirichlet BCs have a structural instability.

In the case of high reflectivities we detected a robust stability under changes of the activation threshold or of the albedo parameter. Small deviations from $k=0$ induce a surface term in the Lyapunov functional that tends to weaken slightly the stability of the stationary structure.

In the general case of finite reflectivity, the region in the space of the parameters where the system exhibits a bistable dynamics could be controlled through the albedo parameter.

We conclude that for our extended system, the region of bistability is strongly affected by the reflectivity of the boundaries. The information obtained from the nullclines can be applied only in the Neumann case ($k=0$). When the reflectivity decreases, we find a restriction in the allowed values of the parameters for which the dynamics is bistable. Neumann BCs produce the more robust patterns for the system we have considered.

ACKNOWLEDGMENTS

The authors would like to thank L. Petcoff for a critical reading of the manuscript, and H. Wio and R. Deza for fruitful discussions. Support from CONICET, Argentina, is acknowledged. G.G.I. is a Fellow of CONICET; C.H.B. is a Member of CONICET.

REFERENCES

1. G. Nicolis and I. Prigogine, *Self-Organization in Nonequilibrium Systems* (Wiley, New York, 1976).
2. P. C. Fife, *Mathematical Aspects of Reacting and Diffusing Systems* (Springer-Verlag, Berlin, 1979).
3. P. C. Fife, Current topics in reaction-diffusion systems, in *Nonequilibrium Cooperative Phenomena in Physics and Related Fields*, M. G. Velarde, ed. (Plenum Press, New York, 1984).
4. M. C. Cross and P. C. Hohenberg, *Rev. Mod. Phys.* **65**:851 (1993).
5. E. Meron, *Phys. Rep.* **218**:1 (1992).
6. G. Nicolis, T. Erneux, and M. Herschkowitz-Kaufman, Pattern formation in reacting and diffusing systems, in *Advances in Chemical Physics*, Vol. 38, I. Prigogine and S. Rice, eds. (Wiley, New York, 1978).
7. A. S. Mikhailov, *Foundations of Synergetics I* (Springer-Verlag, Berlin, 1990).
8. J. D. Murray, *Mathematical Biology* (Springer-Verlag, Berlin, 1985).
9. H. S. Wio, *An Introduction to Stochastic Processes and Nonequilibrium Statistical Physics* (World Scientific, Singapore, 1994).
10. C. Schat and H. S. Wio, *Physica A* **180**:295 (1992).
11. S. A. Hassan, M. N. Kuperman, H. S. Wio, and D. H. Zanette, *Physica A* **206**:380 (1994).
12. S. A. Hassan, D. H. Zanette, and H. S. Wio, *J. Phys. A* **27**:5129 (1994).
13. D. Zanette, H. Wio, and R. Deza, *Phys. Rev. E* **52**:129 (1995).
14. H. S. Wio, G. Izús, O. Ramírez, R. Deza, and C. Borzi, *J. Phys. A:Math. Gen.* **26**:4281 (1993).
15. G. Izús, R. Deza, O. Ramírez, H. Wio, D. Zanette, and C. Borzi, *Phys. Rev. E* **52**:129 (1995).
16. G. Izús, H. Wio, J. Reyes de Rueda, O. Ramírez, and R. Deza, *Int. J. Mod. Phys. B* **10**:1273 (1996).
17. G. Izús, R. Deza, H. Wio, and C. Borzi, *Phys. Rev. E* **55**:4005 (1997).
18. G. Izús, R. Deza, C. Borzi, and H. Wio, *Physica A* **237**:135 (1997).
19. N. G. Van Kampen, *Stochastic Processes in Physics and Chemistry* (North Holland, Amsterdam, 1984).
20. T. Boddington, P. Gray, and C. Wake, *Proc. R. Soc. Lond. A* **357**:403 (1977).
21. S. P. Fedotov, *Phys. Lett. A* **176**:220 (1993).
22. V. Castet, E. Dulos, J. Boissonade, and P. de Keeper, *Phys. Rev. Lett.* **64**:2953 (1990).
23. Q. Ouyang and H. Swinney, *Nature* **352** (1991).
24. G. Nicolis, *Introduction to Nonlinear Science* (Cambridge University Press, Cambridge, 1995).
25. G. Izús, O. Ramírez, R. Deza, and H. Wio, *J. Chem. Phys.* **105**:10424 (1996).
26. B. Ross and J. D. Lister, *Phys. Rev. A* **15**:1246 (1977).
27. R. Landauer, *Phys. Rev. A* **15**:2117 (1977).
28. D. Bedeaux, P. Mazur, and R. A. Pasmantier, *Physica A* **86**:355 (1977).
29. D. Bedeaux and P. Mazur, *Physica A* **105**:1 (1981).
30. W. J. Skocpol, M. R. Beasley, and M. Tinkham, *J. Appl. Phys.* **45**:4054 (1974).
31. H. L. Frisch, Some recent exact solutions of the Fokker-Planck equation, in *Non-Equilibrium Statistical Mechanics in One Dimension*, V. Privman, ed. (Cambridge University Press, Cambridge, 1996), Chapter XVII.
32. H. L. Frisch, V. Privman, C. Nicolis, and G. Nicolis, *J. Phys. A* **23**:1147 (1990).
33. V. Privman and H. L. Frisch, *J. Chem. Phys.* **94**:8216 (1991).
34. B. Von Haefen, G. Izús, R. Deza, and C. Borzi, *Phys. Lett. A*, in press.

35. A. C. Scott, *Rev. Mod. Phys.* **47**:47 (1975).
36. R. Graham, *Lecture Notes in Physics*, Vol. 84 (Springer-Verlag, Berlin, 1978).
37. R. Graham and T. Tel, *Phys. Rev. A* **42**:4661 (1990).
38. R. Graham, Weak noise limit and nonequilibrium potentials of dissipative dynamical systems, in *Instabilities and Nonequilibrium Structures*, E. Tirapegui and D. Villarroel, eds. (Reidel, Dordrecht, 1987).
39. M. Kerszberg, *Phys. Rev. A* **28**:1198 (1983).
40. M. de la Torre and I. Rehberg, *Phys. Rev. A* **42**:2096, 5998 (1990).
41. J. Viñals, E. Hernandez-Garcia, M. San Miguel, and R. Toral, *Phys. Rev. A* **44**:1123 (1991).
42. E. Hernandez-Garcia, J. Viñals, R. Toral, and M. San Miguel, *Phys. Rev. Lett.* **70**:3576 (1993).
43. P. Jung, *Phys. Rep.* **234**:175 (1993).